



# Chemical reactivation of resin-embedded pHuji adds red for simultaneous two-color imaging with EGFP

WENYAN GUO,<sup>1,2</sup> XIULI LIU,<sup>1,2</sup> YURONG LIU,<sup>1,2</sup> YADONG GANG,<sup>1,2</sup> XIAOBIN HE,<sup>3</sup> YAO JIA,<sup>1,2</sup> FANGFANG YIN,<sup>1,2</sup> PEI LI,<sup>1,2</sup> FEI HUANG,<sup>1,2</sup> HONGFU ZHOU,<sup>1,2</sup> XIAOJUN WANG,<sup>1,2</sup> HUI GONG,<sup>1,2</sup> QINGMING LUO,<sup>1,2</sup> FUQIANG XU,<sup>1,2,3</sup> AND SHAOQUN ZENG<sup>1,2\*</sup>

<sup>1</sup>Britton Chance Center for Biomedical Photonics, Wuhan National Laboratory for Optoelectronics-Huazhong University of Science and Technology, 1037 Luoyu Road, Wuhan 430074, China

<sup>2</sup>Department of Biomedical Engineering, Key Laboratory for Biomedical Photonics of Ministry of Education, Huazhong University of Science and Technology, 1037 Luoyu Road, Wuhan 430074, China

<sup>3</sup>State Key Laboratory of Magnetic Resonance and Atomic and Molecular Physics, Brain Research Center, Wuhan Institute of Physics and Mathematics, Chinese Academy of Sciences, West No.30 Xiao Hong Shan, Wuhan 430071, China

\*sqzeng@mail.hust.edu.cn

**Abstract:** The pH-sensitive fluorescent proteins enabling chemical reactivation in resin are useful tools for fluorescence microimaging. EGFP or EYFP is good for such applications. For simultaneous two-color imaging, a suitable red fluorescent protein is an urgent need. Here a pH-sensitive red fluorescent protein, pHuji, is selected and verified to remain pH-sensitive in HM20 resin. We observe 183% fluorescence intensity of pHuji in resin-embedded mouse brain and 29.08-fold fluorescence intensity of reactivated pHuji compared to the quenched state. pHuji and EGFP can be quenched and chemically reactivated simultaneously in resin, thus enabling simultaneous two-color micro-optical sectioning tomography of resin-embedded mouse brain. This method may greatly facilitate the visualization of neuronal morphology and neural circuits to promote understanding of the structure and function of the brain.

© 2017 Optical Society of America

**OCIS codes:** (170.3880) Medical and biological imaging; (160.2540) Fluorescent and luminescent materials; (180.2520) Fluorescence microscopy; (110.4190) Multiple imaging.

## References and links

1. K. D. Micheva and S. J. Smith, "Array tomography: a new tool for imaging the molecular architecture and ultrastructure of neural circuits," *Neuron* **55**(1), 25–36 (2007).
2. R. Y. Tsien, "The green fluorescent protein," *Annu. Rev. Biochem.* **67**(1), 509–544 (1998).
3. H. Xiong, Z. Zhou, M. Zhu, X. Lv, A. Li, S. Li, L. Li, T. Yang, S. Wang, Z. Yang, T. Xu, Q. Luo, H. Gong, and S. Zeng, "Chemical reactivation of quenched fluorescent protein molecules enables resin-embedded fluorescence microimaging," *Nat. Commun.* **5**, 3992 (2014).
4. A. Li, H. Gong, B. Zhang, Q. Wang, C. Yan, J. Wu, Q. Liu, S. Zeng, and Q. Luo, "Micro-optical sectioning tomography to obtain a high-resolution atlas of the mouse brain," *Science* **330**(6009), 1404–1408 (2010).
5. T. Zheng, Z. Yang, A. Li, X. Lv, Z. Zhou, X. Wang, X. Qi, S. Li, Q. Luo, H. Gong, and S. Zeng, "Visualization of brain circuits using two-photon fluorescence micro-optical sectioning tomography," *Opt. Express* **21**(8), 9839–9850 (2013).
6. H. Gong, S. Zeng, C. Yan, X. Lv, Z. Yang, T. Xu, Z. Feng, W. Ding, X. Qi, A. Li, J. Wu, and Q. Luo, "Continuously tracing brain-wide long-distance axonal projections in mice at a one-micron voxel resolution," *Neuroimage* **74**, 87–98 (2013).
7. J. Yuan, H. Gong, A. Li, X. Li, S. Chen, S. Zeng, and Q. Luo, "Visible rodent brain-wide networks at single-neuron resolution," *Front. Neuroanat.* **9**, 70 (2015).
8. H. Gong, D. Xu, J. Yuan, X. Li, C. Guo, J. Peng, Y. Li, L. A. Schwarz, A. Li, B. Hu, B. Xiong, Q. Sun, Y. Zhang, J. Liu, Q. Zhong, T. Xu, S. Zeng, and Q. Luo, "High-throughput dual-colour precision imaging for brain-wide connectome with cytoarchitectonic landmarks at the cellular level," *Nat. Commun.* **7**, 12142 (2016).
9. T. W. Quan, H. Zhou, J. Li, S. W. Li, A. Li, Y. X. Li, X. H. Lv, Q. M. Luo, H. Gong, and S. Q. Zeng, "NeuroGPS-Tree: automatic reconstruction of large-scale neuronal populations with dense neurites," *Nat Methods* **13**(1), 51 (2016).

10. M. Tantama, Y. P. Hung, and G. Yellen, "Imaging intracellular pH in live cells with a genetically encoded red fluorescent protein sensor," *J. Am. Chem. Soc.* **133**(26), 10034–10037 (2011).
11. Y. Li and R. W. Tsien, "pHTomato, a red, genetically encoded indicator that enables multiplex interrogation of synaptic activity," *Nat. Neurosci.* **15**(7), 1047–1053 (2012).
12. N. C. Shaner, M. Z. Lin, M. R. McKeown, P. A. Steinbach, K. L. Hazelwood, M. W. Davidson, and R. Y. Tsien, "Improving the photostability of bright monomeric orange and red fluorescent proteins," *Nat. Methods* **5**(6), 545–551 (2008).
13. Y. Shen, M. Rosendale, R. E. Campbell, and D. Perrais, "pHuji, a pH-sensitive red fluorescent protein for imaging of exo- and endocytosis," *J. Cell Biol.* **207**(3), 419–432 (2014).
14. N. R. Gandasi, K. Vestö, M. Helou, P. Yin, J. Saras, and S. Barg, "Survey of Red Fluorescence Proteins as Markers for Secretory Granule Exocytosis," *PLoS One* **10**(6), e0127801 (2015).
15. S. Sankaranarayanan, D. De Angelis, J. E. Rothman, and T. A. Ryan, "The use of pHluorins for optical measurements of presynaptic activity," *Biophys. J.* **79**(4), 2199–2208 (2000).
16. S. J. Gray, V. W. Choi, A. Asokan, R. A. Haberman, T. J. McCown, and R. J. Samulski, "Production of recombinant adeno-associated viral vectors and use in vitro and in vivo administration," *Current Protocols in Neuroscience* / editorial board, Jacqueline N. Crawley ... [et al.] **Chapter 4**(Unit 4 17 (2011)).
17. X. Xiao, J. Li, and R. J. Samulski, "Production of high-titer recombinant adeno-associated virus vectors in the absence of helper adenovirus," *J. Virol.* **72**(3), 2224–2232 (1998).
18. F. Osakada, T. Mori, A. H. Cetin, J. H. Marshel, B. Virgen, and E. M. Callaway, "New rabies virus variants for monitoring and manipulating activity and gene expression in defined neural circuits," *Neuron* **71**(4), 617–631 (2011).
19. I. R. Wickersham, S. Finke, K. K. Conzelmann, and E. M. Callaway, "Retrograde neuronal tracing with a deletion-mutant rabies virus," *Nat. Methods* **4**(1), 47–49 (2007).
20. Y. Gang, H. Zhou, Y. Jia, L. Liu, X. Liu, G. Rao, L. Li, X. Wang, X. Lv, H. Xiong, Z. Yang, Q. Luo, H. Gong, and S. Zeng, "Embedding and Chemical Reactivation of Green Fluorescent Protein in the Whole Mouse Brain for Optical Micro-Imaging," *Front. Neurosci.* **11**, 121 (2017).
21. H. Gong, D. Xu, J. Yuan, X. Li, C. Guo, J. Peng, Y. Li, L. A. Schwarz, A. Li, B. Hu, B. Xiong, Q. Sun, Y. Zhang, J. Liu, Q. Zhong, T. Xu, S. Zeng, and Q. Luo, "High-throughput dual-colour precision imaging for brain-wide connectome with cytoarchitectonic landmarks at the cellular level," *Nat. Commun.* **7**, 12142 (2016).
22. G. R. Newman and J. A. Hobot, "Resins for combined light and electron microscopy: a half century of development," *Histochem. J.* **31**(8), 495–505 (1999).
23. N. C. Shaner, R. E. Campbell, P. A. Steinbach, B. N. Giepmans, A. E. Palmer, and R. Y. Tsien, "Improved monomeric red, orange and yellow fluorescent proteins derived from *Discosoma* sp. red fluorescent protein," *Nat. Biotechnol.* **22**(12), 1567–1572 (2004).
24. A. S. Mishin, V. V. Belousov, K. M. Solntsev, and K. A. Lukyanov, "Novel uses of fluorescent proteins," *Curr. Opin. Chem. Biol.* **27**, 1–9 (2015).

## 1. Introduction

To visualise the refined 3D structure of thick biological tissues, it usually depends on resin embedding and subsequent array tomography [1]. But the fluorescent proteins for labelling are prone to be damaged or quenched in resins, especially in hydrophobic resins [2]. According to our previous report, the enhanced green fluorescent protein (EGFP) or enhanced yellow fluorescent protein (EYFP) improved from GFP in jellyfish was just quenched instead of being damaged by resin and could be chemically reactivated [3]. The fluorescence of pH-sensitive fluorescent proteins in labeled tissue can be quenched in an acidified resin embedding process by chromophore protonation. This fluorescence quenching in the tissue block can greatly lower the background fluorescence in wide-field imaging. Thus, the strong out-of-focus interference in wide-field imaging is avoided via chemical reactivation of surface layer fluorescence. Combining the fluorescent proteins labeling, resin embedding and fluorescence micro-optical sectioning tomography (fMOST) [4, 5], much work was done to visualize the neuronal morphology and neural circuits at brain-wide scale [6–9].

To understand the structure and function of intact tissues such as the sophisticated mouse brain, simultaneous two-color imaging is of urgent need. Among the *Aequorea Victoria* GFP and its pH sensitive variants, however, it is difficult to find a candidate suitable for two-color chemical reactivation imaging with EGFP since these fluorescent proteins are either not bright enough or cross-color with EGFP. So a bright pH-sensitive red fluorescent protein is of urgent need. Fortunately, there are many reported pH-sensitive red fluorescent proteins including pHRed [10], pHTomato [11], mOrange2 [12] and pHuji [13] and so on.

The pHRed is quenched in alkaline solutions, while EGFP or EYFP is activated in alkaline solutions. So it is infeasible to use pHRed for simultaneous two-color chemical reactivation imaging in conjunction with EGFP or EYFP. The pHTomato, mOrange2 and pHuji all are quenched in acidic solutions and reactivated in alkaline solutions. With the change of pH, the fluorescence intensity alters more greatly for pHuji than pHTomato. The mOrange2 retains some of its fluorescence in acidic solutions [14] and cannot rapidly change its fluorescence intensity like the SEP [15] with the pH variation. Therefore, we selected pHuji to verify whether it is compatible with resin embedding.

In HM20 resin, we find pHuji remains pH-sensitive and it is bright enough to show the fine architecture of neurites. pHuji and EGFP or EYFP can be quenched simultaneously and chemically reactivated at the same time in resin. Via simultaneous two-color chemical reactivation imaging based on fMOST, both EGFP and pHuji showed similar results for labeling the full morphology of neurons.

## 2. Materials and method

### 2.1 Virus preparation

The gene sequence of pHuji is synthesized and cloned into a vector (Addgene, #20298). Then the recombinant adeno-associated virus (AAV) vector was packaged into AAV viral particles. Some previous reports detailed the classical AAVs production and usage [16, 17]. With serotype 5, promoter EF1a, double floxed inverted open reading frame (DIO), the cellular receptor for subgroup A avian sarcoma and leukemia virus (TVA) gene fragment and pHuji gene, the recombinant AAV was named as the abbreviation “AAV5-EF1a-DIO-TVA-pHuji”. The other AAVs were named in the same manner. The rabies viruses were produced according to the previous protocols [18, 19]. EnvA-pseudotyped SADΔG-EYFP rabies viruses (Rv) were named as Rv-ENVA-EYFP.

### 2.2 Virus injection

Mice were anesthetized with 5% chloral hydrate (0.1 ml per 10 g body weight) and placed in a rodent stereotaxic frame. The stereotaxic coordinates for the target areas were based on the Mouse Brain in Stereotaxic Coordinates Atlas. The AAVs were used as anterograde tracers. The craniotomy was made using anterior-posterior (AP) coordinates from bregma (in mm), medio-lateral (ML) coordinates from midline and dorso-ventral (DV) coordinates from the brain surface. AAV5-EF1a-DIO-TVA-pHuji was mixed to 300 times diluted AAV2-pgk-Cre with a proportion of 2:1. Then 300 nl mixed AAVs were injected to mice M1 motor cortex with stereotaxic coordinates for AP, 1.0, ML, -1.5, DV, -1.5. Thirty days later, some of the mice were injected with 100 nl Rv-ENVA-EYFP at the same site respectively and were raised for another 12 days before transcardial perfusion. The rest of the mice were transcardially perfused after another 2 days. For two-color fMOST, the LSL-Flpo mice (JAX stock number 028584) were injected with 20 nl CAV-Cre at CPU (AP, 1.0, ML, 2.0, DV, -3.4), 50 nl AAV8-fDIO-TVA-EGFP at M1 (AP, 1.0, ML, 1.5, DV, -1.5), 50 nl AAV5-EF1a-DIO-TVA-pHuji at M2 (AP, 1.3, ML, 0.75, DV, -1.25). 45 days later, the mice were transcardially perfused and the brains were embedded by HM20 for fMOST imaging. All the animal experiments followed procedures approved by the Institutional Animal Ethics Committee of Huazhong University of Science and Technology.

### 2.3 Resin embedding

The procedures were performed according to the previous report [20] with some modifications. In brief, the mouse brains or brain slices were embedded with Lowicryl HM20 Resin Kit. Post fixation with 4% PFA for about 12 h. The samples were washed in 0.01M PBS five times (4 h each) and dehydrated in ethanol/ddH<sub>2</sub>O series: 50%, 75%, 95%, 100%, 100%, 100%; 2 h each. Followed by immersion in xylene for three times, 2 h each. After

transparency, the samples were infiltrated in HM20 working solution/xylene series: 50%, 75%, 100%, 100%, 100%; 2 h each for the first three series and 12 h each for the last two series. All the wash, dehydration and infiltration steps were carried out at 4°C. Each of HM20 working solution consisted of 0.064 g azobisisobutyronitrile (AIBN), 7 g crosslinker and 33 g monomer. The crosslinker and the monomer of HM20 should be filtered by aluminium oxide packed column before use. After infiltration, the samples were kept in a vacuum drying oven in dark at 37°C for 8 h, 45°C for 8 h and 50°C for 3 h to polymerize completely.

## 2.4 Imaging

For commercial microscope imaging, the brain slices with thickness of 100  $\mu\text{m}$  were mounted onto the glass slides and the images were generated by Zeiss 710 confocal microscope. According to the morphology of neurites, the somas shape, location and other landmarks of the slice coronal plane, the same regions could be found and imaged after different treatments. For fMOST imaging, the procedures were performed according to the previous reports [4, 5, 21]. Briefly, the embedded brain was immersed in a water bath containing 0.1 M  $\text{Na}_2\text{CO}_3$  solution. The water bath was fixed on a 3D translation stage in the wide-field large-volume tomography (WVT). The sectioning (surface cutting) was achieved through a relative motion between the fixed diamond knife and the 3D translation stage. The EGFP or EYFP was excited by a 488-nm laser and the pHuji was excited by a 561-nm laser. Since the fields of view in the two channels were imaged simultaneously, no extra two-channel registration was needed.

## 3. Results

To find a pH-sensitive red fluorescent protein for dual-color chemical reactivation imaging by fMOST, we selected pHuji as a candidate. According to the reported photophysical properties of pHuji (Table 1) [13], it has no cross-color interference with EGFP and is hopeful for dual-color chemical reactivation imaging. But whether these properties of pHuji remain in hydrophobic resin is unknown. So firstly we tested whether pHuji remained pH-sensitive in the commonly used resin HM20.

**Table 1. Photophysical properties of pHuji and EGFP**

Fluorescent proteins	Brightness (Times of EGFP)	pKa	Excitation peak (nm)	Emission peak (nm)	pH-dependent change of fluorescence intensity
pHuji	1.1	7.7	566	598	larger
EGFP	1	5.9	489	509	large

We injected two mixed AAVs, AAV5-EF1a-DIO-TVA-pHuji and AAV2-pgk-Cre, to a C57BL/6 mouse brain by stereotaxic injection. 32 days later, the mouse was perfused and the brain was sectioned with thickness of 100  $\mu\text{m}$ . Then some of the brain slices were embedded by the acidic HM20 resin. We found pHuji was bright enough to label the full morphology of neurons before HM20 embedding [Fig. 1(a)]. In the acidifying HM20 resin with pH = 5.0, pHuji was quenched almost completely since there was very weak red fluorescence observed only in somas and in thick neurites near somas [Fig. 1(b)]. When the fluorescence quenched brain slices were immersed into 0.1M  $\text{Na}_2\text{CO}_3$  solution (pH = 11.7), we observed very bright reactivated red fluorescence under the microscope [Fig. 1(c)]. These results indicate pHuji remains pH-sensitive in HM20 resin and may be compatible with chemical reactivation imaging. In particular, pHuji was bright enough in resin to show the fine architectures of neurites, such as dendritic spines and axon boutons [Fig. 1(d)].

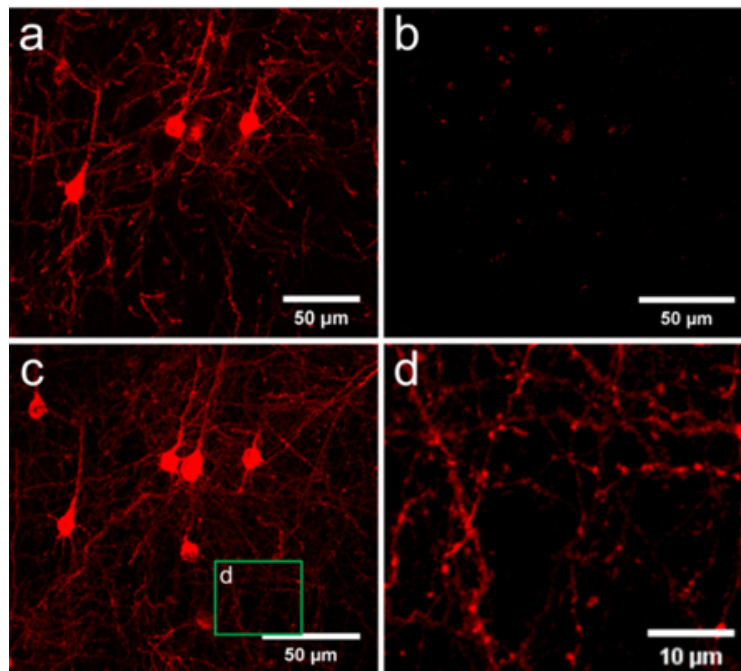


Fig. 1. The pHuji is pH-sensitive in HM20 resin. (a) pH = 11.7. (b) pH = 5.0. (c) pH = 11.7. (d) Enlargements of insets (green boxes) from (c). The somas were located in primary motor cortex (M1). Scale bars as indicated.

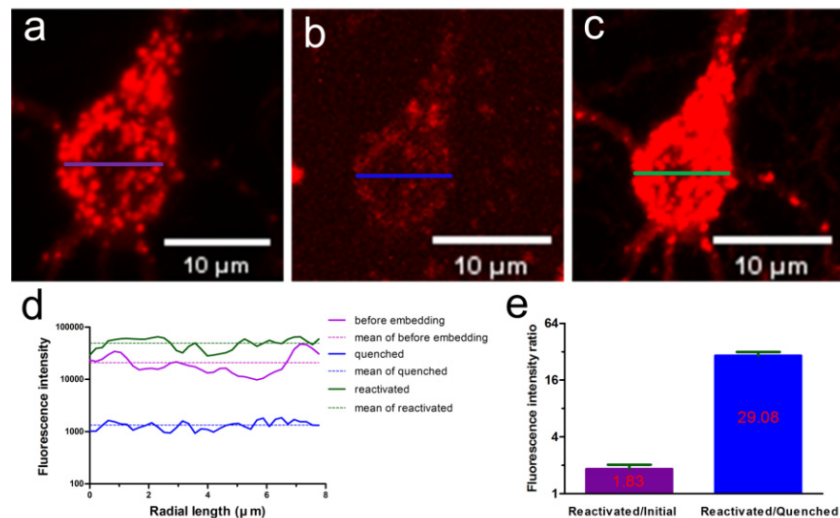


Fig. 2. Chemical reactivation of pHuji in a HM20-embedded mouse brain slice. (a) A neuronal soma before HM20 embedding, with pH = 11.7. (b) The same neuronal soma after HM20 embedding, with pH = 5.0. (c) The same neuronal soma after HM20 embedding, with pH = 11.7. (d) The gray values along radial length of the neuronal soma showed in (a), (b), (c). (e) The fluorescence intensity ratio of five neuronal somas at different states of pHuji. The somas were located in primary motor cortex (M1). Scale bars as indicated.

Further, we quantitatively analyzed the increased fluorescence intensity of reactivated pHuji [Fig. 2(c)] compared to the quenched state [Fig. 2(b)] or the initial state before resin embedding [Fig. 2(a)]. We compared the mean gray values along radial length of five



neuronal somas labeled by pHuji at initial, quenched or reactivated states [Fig. 2(d) shows a typical one], and found  $29.08 \pm 5.41$ -fold fluorescence intensity of reactivated pHuji compared to the quenched state,  $1.83 \pm 0.40$ -fold compared to the initial state before HM20 embedding [Fig. 2(e)]. The embedding induced tissue shrinkage and higher refractive index may contribute to the increased fluorescence intensity of embedded pHuji in comparison to the non-embedded pHuji. These results indicate most of the pHuji molecules are just quenched instead of being damaged directly, and can be reactivated as long as the surrounding chemical conditions are suitable.

Since pHuji was selected for simultaneous two-color chemical reactivation imaging plus EGFP, we then tested whether pHuji and EGFP could quench and reactivate simultaneously in resin. Similarly, AAV5-EF1a-DIO-TVA-pHuji and AAV2-pgk-Cre mixtures were injected to the C57BL/6 mouse brains. 30 days later, Rv-ENVA-EYFP viruses were injected to the same site of the mouse brains. After another 12 days, the mice were perfused and the brain slices with dual-color labeling were selected. Around the injection site, we could see the initial neurons coinfecting by the AAV and the rabies virus [Fig. 3(d)], as well as mono-trans-synaptic neurons infected by Rv. In the alkaline PBS solution (pH 9.0) before HM20 embedding, both pHuji and EYFP are bright enough to show the neurites [Fig. 3(a)]. When embedded in acidic HM20 (pH = 4.5), besides the background noise indicating the injection site, almost no fluorescence was seen in cells [Fig. 3(b)]. However, when the embedded brain slices were soaked in alkaline PBS solution (pH = 9.0) for several minutes, the fluorescence of both pHuji and EYFP was recovered rapidly and completely at the same time [Fig. 3(c)]. Since EYFP and EGFP are very similar in photophysical properties, our results may imply pHuji can quench and reactivate simultaneously with EGFP or EYFP.

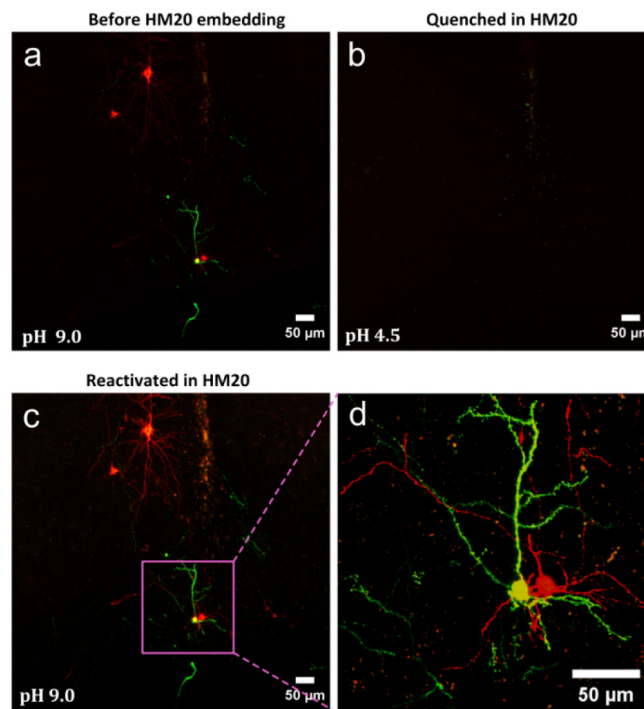


Fig. 3. The pHuji and EYFP quenched and reactivated simultaneously in HM20 resin. (a) pH = 9.0 before HM20 embedding. (b) pH = 4.5 after HM20 embedding. (c) pH = 9.0 after HM20 embedding. (d) A close up view of the inset from (c). The somas were located in primary motor cortex (M1). Scale bars as indicated.

We further demonstrate the simultaneous chemical reactivation of EGFP and pHuji is suitable for fMOST to visualize the neuronal morphology and neural circuits. Via labeling by AAV mediated overexpression of EGFP or pHuji, fMOST imaging revealed the dense dendrites and spines near the somas [Fig. 4(a), 4(c)] and the axons and axon boutons [Fig. 4(b), 4(d)] far away from the somas very clearly. Obviously, pHuji performed nearly as well as EGFP, though the 561-nm channel had higher background fluorescence [Fig. 4(d)]. These results indicate pHuji, as well as EGFP, has the ability to label the fine architecture of neurites, especially long-distance axonal projections, for brain-wide tracing of continuous neuronal pathways.

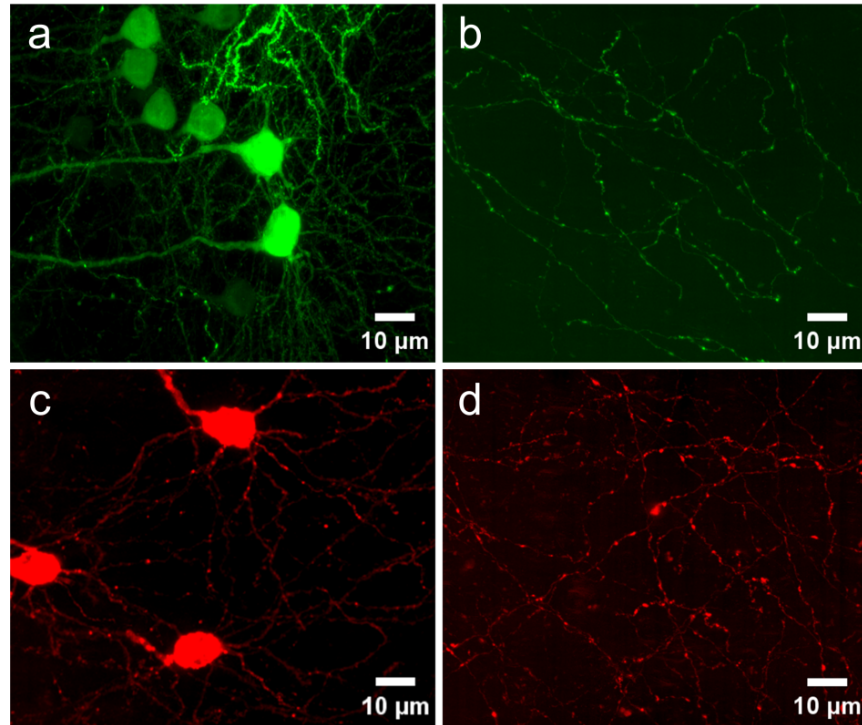


Fig. 4. Simultaneous chemical reactivation of EGFP and pHuji imaged by fMOST. (a) The neuronal somas and nearby dendrites labeled by EGFP. (b) The axons and axon boutons far away from somas labeled by EGFP. (c) The neuronal somas and nearby dendrites labeled by pHuji. (d) The axons and axon boutons far away from somas labeled by pHuji. The somas labeled by EGFP were located in primary motor cortex (M1) while those labeled by pHuji were located in secondary motor cortex (M2). Scale bars as indicated.

#### 4. Discussion and conclusions

Resin embedding is a vital sample processing method of thick biological tissues imaged by electron microscope or optical microscope [22]. The fluorescent protein labeling technique including GFP and its variants was proved to be compatible with resin embedding in our previous report [3]. To find a pH sensitive red fluorescent protein for simultaneous two-color imaging, among the pH-sensitive red fluorescent proteins derived not from GFP, we selected pHuji [13], a bright red fluorescent protein developed in 2014 that can provide in situ pH-dependent changes in fluorescence intensity. We found pHuji remained pH-sensitive in resin and could be quenched and reactivated simultaneously with EGFP or EYFP. Similar to GFP and all its pH sensitive mutants, most of pHuji molecules were quenched instead of being damaged in resin. And the fluorescence in the surface layer of the tissue block could be chemically reactivated by alkaline solutions. So a fast and high-resolution wide-field imaging

based on chemical reactivation was achieved by using pHuji instead of pH-insensitive fluorescent proteins.

To our knowledge, pHuji is the first pH-sensitive red fluorescent protein which is proved to be compatible with hydrophobic resin embedding. The indirect precursor of pHuji, mOrange [23], has a chromophore surrounded by a stable  $\beta$ -barrel structure [24], which is similar to the  $\beta$ -barrel in GFP. Very likely pHuji also has such a structure, which may protect it from being damaged by resin embedding. The optimal excitation wavelength for pHuji is 566 nm, with emission peak at 598 nm, which is longer than the emission peak of EGFP for about 89 nm. So it is very suitable for simultaneous two-color imaging using pHuji plus EGFP.

Although pHuji is more prone to photobleaching than EGFP, and the 561-nm channel has relative higher background fluorescence, in combination with EGFP or EYFP, pHuji enables simultaneous dual-color chemical reactivation imaging of resin embedded thick tissues for the first time. Finding a good alternative to pHuji or a better mutant of mApple may improve the light stability. Updating imaging method with decreased background or photobleaching may provide another way to improve two-color chemical reactivation imaging. So there are reasons to believe that, simultaneous two-color chemical reactivation imaging will have great opportunities for the visualization of neuronal morphology and neural circuits.

### Funding

Program 973 (2015CB755603).

### Acknowledgment

We would like to thank some other members of Britton Chance Center for Biomedical Photonics for providing advice and other help. Portions of this work were presented at the {Asia Communications and Photonics Conference} in {2016}, {AS3I.2}.

### Disclosures

The authors declare that there are no conflicts of interest related to this article.